

Energies for Cyclic and Acyclic Aggregations of Adamantane Sharing Six-membered Rings

Alexandru T. Balaban,* Yenni P. Ortiz, Douglas J. Klein, Debojit Bhattacharya

Texas A&M University at Galveston, 200 Seawolf Parkway, Galveston, TX 77553, USA

* Corresponding author's e-mail address: balabana@tamug.edu

RECEIVED: December 12, 2016 * REVISED: February 20, 2017 * ACCEPTED: February 22, 2017

THIS PAPER IS DEDICATED TO PROFESSOR NENAD TRINAJSTIĆ ON THE OCCASION OF HIS 80TH BIRTHDAY

Abstract: Tension energies for acyclic and cyclic assemblies of adamantane units sharing hexagons of carbon atoms converge in a size-extensive manner for large numbers n of adamantane units. In most cases the convergence features diagrams of strain energy per adamantane unit E (n^{-1}) versus n^{-2} for cyclic aggregates and versus n^{-1} for acyclic aggregates having linear dependence with slopes of opposite signs. However, we found two exceptions which are discussed in the present paper, with convergence involving linear dependence with slopes of the same sign.

Keywords: polymantanes, diamondoids, tension, stress.

INTRODUCTION

SINCE their discovery in petroleum, diamond hydrocarbons (diamantoids) have gained eminence due to the possibility of isolating and purifying them.^[1–3] They are the most stable among all their valence isomers because all their C–C bonds are in staggered conformation. Further prominence arises because of their exceptional strength and stability, as possibilities to construct robust nanomachines. But especially in contemplated^[4] designs involving circular nanostructures (e.g. wheels or gears) there should be notable stresses and strains – so that the investigation of such in polymantane-based materials should be appropriate. The 2016 Chemistry Nobel Prize to Jean-Pierre Sauvage, Sir J. Fraser Stoddart and Bernard L. Feringa for their design and production of molecular machines stresses this statement. And it should be an area of interest to Nenad Trinajstić.

In a previous paper (which will be considered to be Part 1, whereas the present paper can be considered to be Part 2 this series) were presented acyclic and cyclic strings of adamantane or diamantane cells that shared vertices, edges, or 6-membered rings.^[5] In order to provide information without needing to consult Part 1, some repetition of text and figures from Part 1 is made.

Hydrogen-depleted formulas are used in the following unless otherwise stated. Diamondoids consist of adamantane units or cells sharing vertices, edges, or 6-membered carbon rings. They are partially characterized by their constitutional (molecular) formulas, and uniquely characterized by their structural formulas. When pairs of adamantane units share a chair-shaped 6-membered “face” they are called polymantanes. By inscribing a virtual vertex in the center of each unit, and connecting vertices corresponding to adjacent cells, one obtains the inner dual (*i. e.* dualist) which also characterizes uniquely the polymantane. In the present context, *the terms “cyclic” and “acyclic” will refer to the dualist.* Polymantanes occur in three common kinds: catamantanes when the dualist is acyclic; perimantanes when the dualist contains six-membered rings; and coronamantanes when the dualist has larger rings which are not peripheries of “internal” six-membered ring aggregates. To specify polymantane structures, Balaban and Schleyer proposed a concise notation describing the dualist.^[6] A similar proposal applied to polycyclic condensed benzenoid hydrocarbons (catafusenes, perifusenes, and coronafusenes) had been formulated earlier by Balaban and Harary.^[7] Catamantane dualists may be characterized by a sequence of digits (1, 2, 3 and/or 4) specifying the four possible orientations along

tetrahedral directions around each vertex along the longest path of the dualist, choosing among all possibilities the one corresponding to the smallest number formed by reading sequentially all digits from one end of that path to the other end. Branchings are denoted by brackets.

Returning to the analogy with polycyclic cata-condensed benzenoids, when their dualists attain certain dimensions they may connect their endpoints forming cycles and converting catafusenes into perifusenes or coronafusenes. Alternatively, these ends may exit the two-dimensional plane to yield tridimensional helicenes, which are well-known stable compounds. By contrast, there are no real four-dimensional catamantanes, although their imaginary counterparts can be conceptually described. A major difference from polycyclic benzenoids, which on following a path in the benzenoid network the path does not return to its starting position despite the corresponding walk on the honeycomb net so returning – because of the ability of the benzenoid net to twist out of the plane of the honeycomb net – a sort of distortion not available to polymantane structures. Catamantanes are of two types: regular $C_{4n+6}H_{4n+12}$, and irregular if there are fewer hydrogens. If digits 1, 2, 3, and 4 correspond to letters p , q , r , and s , irregular catamantanes have dualists with a sequence of digits of type $p-q-r-p$; in such cases the ends of the dualist come so close together that in order to avoid hydrogen overlap, the C–C bond angles must undergo distortion. Moreover, whenever a sequence $p-q-r-p-q$ would occur by adding successive adamantane cells, a perimantane results automatically with its cyclic dualist which has the digit sequence 12312, equivalent to 123123 because the last edge of the dualist (denoted by digit 3) is inserted to properly accommodate the space available, since there is no fourth dimension!

In the following we discuss three classes of non-branched catamantanes and perimantanes sharing hexagons. The notation for long acyclic catamantanes contains, in square brackets, the repeating unit followed by three dots. To start with catamantanes, their dualists are continuous sequences of straight lines with equal length. It is known that a non-planar sequence of three lines on the diamond lattice is chiral.^[8,9] Indeed, taking as an example the tetramantanes, and ignoring the branched [1(2)3]tetramantane, there are two isomeric regular non-branched tetramantanes: the achiral zigzag [121]tetramantane whose dualist is a z-like coplanar sequence of three equal lines, and the chiral [123]tetramantane with a nonplanar dualist. In the former case one may continue lengthening the dualist in a self-similar manner resulting in a quasi-linear zigzag poly[12...]*catamantane* which is examined in detail in the following. However, in the latter case, there are two possibilities: (i) lengthening the dualist by repeating the 123 triplet, which leads to cancellation of chirality

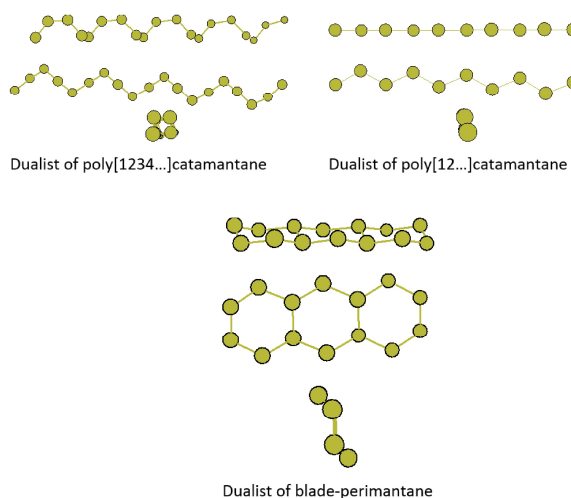


Figure 1. Dualists of diamond hydrocarbons sharing chair-shaped carbon atom hexagons (three views in each case): acyclic regular helix poly[1234...]*catamantane*s, acyclic zigzag poly[12...]*catamantane*s, and acyclic blade-perimantane. Cyclic and acyclic poly[1234...]*catamantane*s were also discussed in Part 1.^[5]

yielding an irregular poly[123...]*catamantane*; and (ii) adding a fourth direction in a self-similar manner, which leads to a regular, helical and chiral poly[1234...]*catamantane*. The latter aggregate had been discussed in Part 1, and will again be examined in detail below. The present paper also includes a new regular catamantane and a perimantane. Figure 1 displays for each type of acyclic polymantane several views of their dualists. As in Part 1, in all following figures, virtual vertices of dualists are colored in olive; quaternary (C), tertiary (CH) and secondary (CH₂) carbon atoms are presented in red, black, and light blue, respectively.

The last aggregate in Figure 1 has a dualist (whose vertices mimic carbon atoms of all-*trans*-perhydro-acene) whose dualist mimics the carbon atoms of the zigzag poly[12...]*catamantane*, the first aggregate in Figure 1. We refer to Schleyer-Williams-Blanchard “strain” energy as the *SWB-tension energy*^[10] delivered by the most recent CambridgeSoft MM2 package that we use. In adamantane this SWB-tension energy amounts to about 6 kcal/mol, despite there being very little identifiable “strain” in terms of anomalous bond lengths or bond angles. Indeed rather than such geometric strain, SWB ascribe^[9] their so-called “strain” energies due to interactions between non-neighbor atoms and bonds. In homologous diamondoids this tension energy increases with the number of adamantane units, and varies among isomeric diamondoids as shown in the following examples. On comparing the three regular isomeric tetramantanes C₂₂H₂₈, SWB-tension

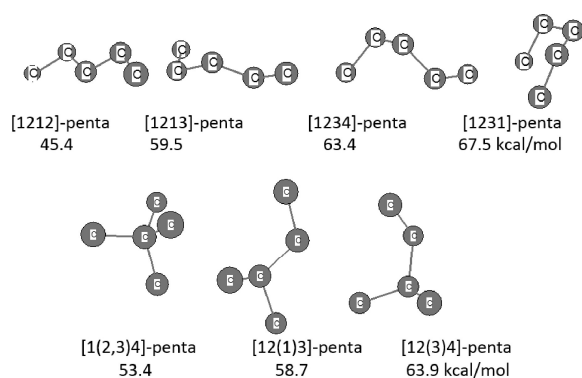


Figure 2. Dualists of pentamantanes with their notation and strain energies: upper row, the three isomeric regular and the unique irregular [1231]-pentamantane. Lower row, the three isomeric branched pentamantanes.

energies are 36.2, 45.1, and 49.9 kcal/mol for [121]-, [1(2)3]- and [123]-tetramantane, respectively. For the regular catapentamantanes $C_{26}H_{32}$, tension energies are 45.4, 53.4, 58.7, 59.5, 63.4, and 63.9 kcal/mol for [1212]-, [1(2,3)4]-, [12(1)3]-, [1213]-, [1234]-, and [12(3)4]-pentamantane respectively. The irregular [1231]-pentamantane $C_{25}H_{32}$ has the highest tension energy of 67.5 kcal/mol. Figure 2 helps in visualizing pentamantanes with the help of their dualists' geometry: here the balls indicate the centers of adamantane units and the edges connect centers of units sharing chair-shaped hexagons of carbon atoms.

It can be seen that a zigzag two-dimensional conformation of the dualist plays the dominant favorable role leading to compactness of the diamondoid, and that branching of dualists (which changes the partition formula) is relatively unimportant, with [1234]-, and [12(3)4]-pentamantane having practically equal strain energies. An unfavorable aspect leading to high strain is the association of large topological distances with low geometrical distances; an extreme example is provided by irregular catamantanes.

Results for various adamantane polymers can be viewed to have total energies or SWB-tension energies approximated in an additive manner. This presumes an energy ϵ_{int} for an internal adamantyl unit and another energy ϵ_{end} for an end (terminal) adamantyl unit. For an open-chain polymer or aggregate, this means that the (SWB-tension) energy for the whole polymer of adamantyl units is:

$$E_n \cong \epsilon_{\text{end}} + (n-2)\epsilon_{\text{in}} + \epsilon_{\text{end}} \quad (1)$$

Or equivalently

$$E_n/n \cong \epsilon_{\text{in}} + \frac{2(\epsilon_{\text{end}} - \epsilon_{\text{in}})}{n} \quad (2)$$

so that a plot of E_n/n versus $1/n$ is expected to be

asymptotically linear, with an intercept equal to ϵ_{in} and a slope which is either positive or negative as $\epsilon_{\text{end}} < \epsilon_{\text{in}}$ or $\epsilon_{\text{in}} < \epsilon_{\text{end}}$. Indeed, there is evidence^[11-14] that such a functional form is highly accurate.

For all cases examined in Part 1, it was found that acyclic aggregates yielded SWB plots with negative slope, meaning that an adamantane end-unit has less net tension than internal units. However, we have continued searching and although most aggregates behaved similarly, we find two counterexamples discussed in the present communication, with plots for both cyclic and acyclic aggregates with positive slope, but still converging for large numbers of adamantane units.

Continuing our "additive" analysis, we see that for n -fold cyclically symmetric structures, there are n equivalent units, each with a common contribution ϵ'_n . But since the units must be geometrically distorted (relative to the open-chain units), there must be some strain, so that ϵ'_n should generally be $> \epsilon_n$. The distortion (or strain) in the bond length and/or bond angles naturally is proportional to $1/n$. If the linear-chain experiences no screw-like torsion along the chain, which is to say it approaches a simple translational symmetry in the interior, then the curvature-induced stress energy should be proportional to the square of this geometric strain. Thus for each of the n units of the polymer there should be an additional contribution γ/n^2 (beyond ϵ_n) to the net SWB-tension energy E'_n , with γ a (positive) curvature-stress parameter. Consequently

$$E'_n/n = \epsilon'_n \cong \epsilon_{\text{in}} + \frac{\gamma}{n^2} \quad (3)$$

so that a plot of E'_n/n versus $1/n^2$ is anticipated to be linear. With the (geometric) strain $\sim 1/n$ measuring deviations from the ideal unstressed case, there can also be higher order curvature-strain corrections in $1/n$ (say $\sim 1/n^3$ or $\sim 1/n^4$). If there were to be a screw-like torsion in the open-chain case, and this is "straightened out" in going to the cyclic chain, then there would be an additional correction Δ to ϵ'_n , so that

$$E'_n/n = \epsilon'_n \cong \epsilon_{\text{in}} + \frac{\gamma}{n^2} + \Delta$$

with $\Delta > 0 < \gamma$. Here γ/n is a genuine net strain-energy contribution to the overall tension energy E'_n .

The following separate sections deal with three classes of polymantanes sharing hexagons of carbon atoms. The 1st section repeats, in abbreviated form, data from Part 1 but without repeating the corresponding tables which appeared in Part 1.

Regular Helix Poly[1234...]catamantanes

Diamantane results from two adamantane units sharing a "face" of chair-shaped hexagon of carbon atoms, and

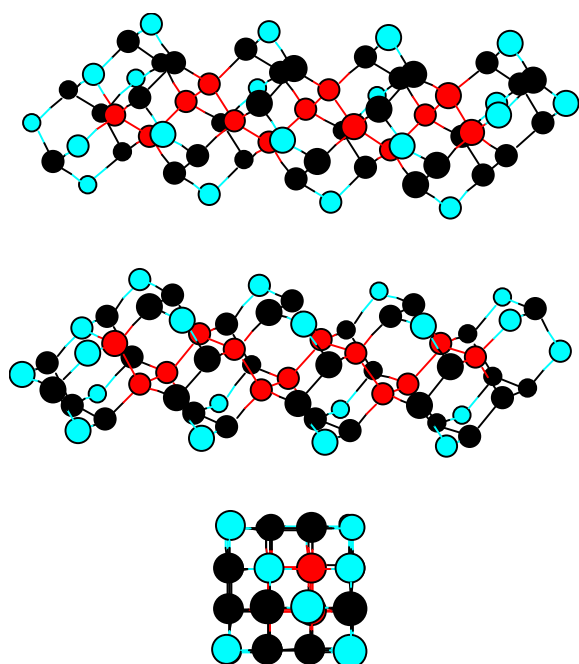


Figure 3. Three views of a fragment with 4 diamantane and 8 adamantane cells for the acyclic regular acyclic helix poly[1234...]catamantane without its dualist.

higher catamantanes proceed with further face-sharings. In this section, we study linear-chain and cyclic helical cata-condensed aggregates of adamantane units sharing hexagons, but with the building units based on (face-sharing) fusions of diamantane units, conserving their reciprocal orientation.

Figure 3 shows a small portion of such an acyclic helix (from front and side views). In the middle front view of

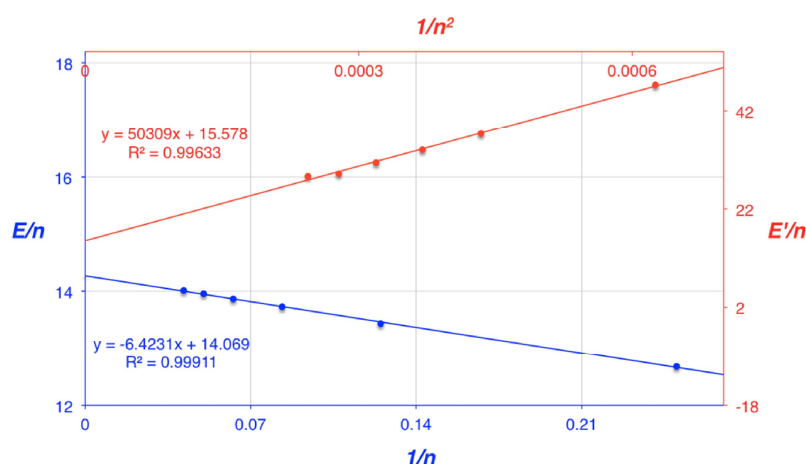


Figure 4. SWB-Tension energies (in kcal/mol) per adamantane unit for helix- n -adamantanes. The upper plot in red for cyclo[1234]-helix- n -adamantanes is for the SWB-tension energy per unit versus n^{-2} , while the lower plot for acyclic [1234]-helix- n -adamantanes, in blue is for the SWB-tension energy per unit versus n^{-1} . The structure illustrations are for cyclo[1234]-helix-10-diamantane, and acyclic [1234]-helix-6-diamantane (with color codes as in Figure 1).

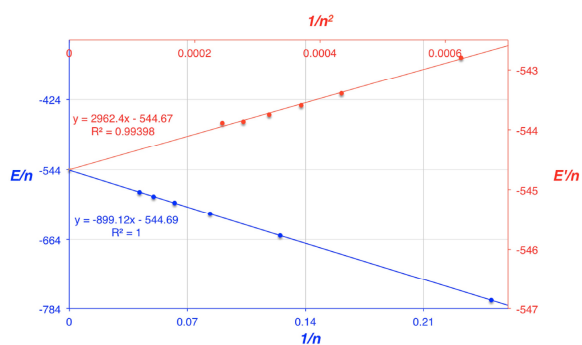


Figure 5. Total energies (in eV) per adamantane unit for [1234]-helix- $[n]$ adamantanes. The upper plot in red for cyclo[1234]-helix- $[n]$ adamantanes is for energies versus n^{-2} , while the lower plot in blue for acyclic [1234]-helix- $[n]$ adamantanes is for energies versus n^{-1} .

Figure 3, one sees that four adamantane units, or two diamantane units, make up one turn of the helix. The IUPAC (von Baeyer) nomenclature of such aggregates was discussed earlier, though we use the Balaban-Schleyer notation for catamantanes (as is based on dualists, with digits 1,2,3,4 identifying the four possible directions of bonds around sp^3 -hybridized carbon atoms). One of the three isomeric tetramantanes, the chiral [123]tetramantane, is the precursor of the chiral helical systems discussed here.

For an acyclic n -adamantane chain, the overall molecular formula is $C_{4n+6}H_{4n+12}$, and the partitioned formula is $C_{n-2}(CH)_{2n+4}(CH_2)_{n+4}$. For cyclic chains, the corresponding overall and partitioned formulas are $C_{4n}H_{4n}$ and $C_n(CH)_{2n}(CH_2)_n$.

In Figures 4 and 5 one can see the variation of the

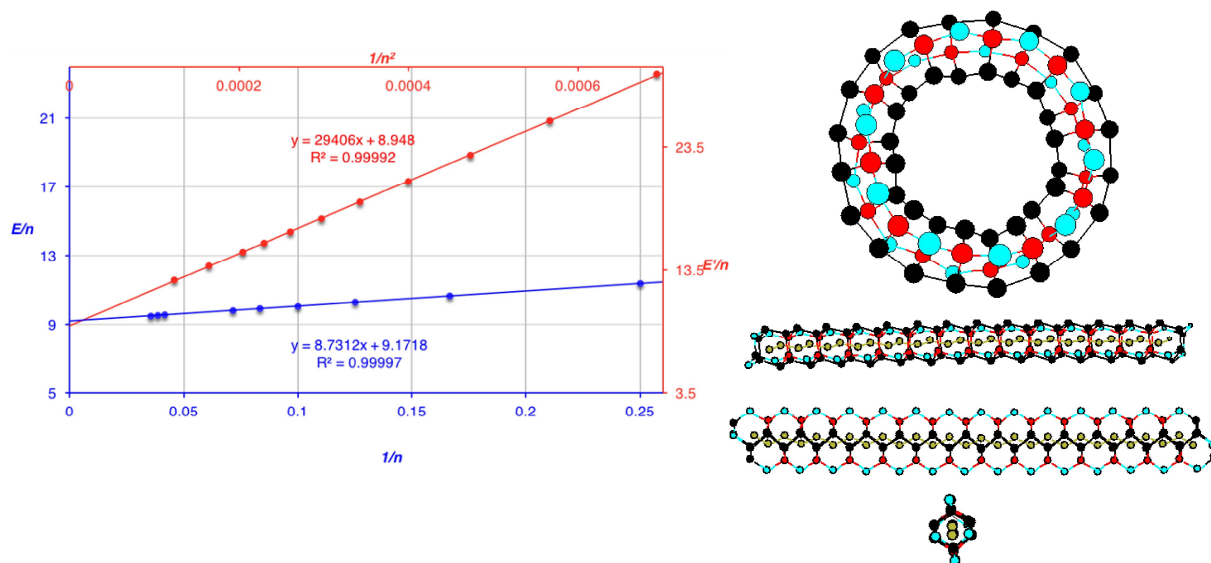


Figure 6. zz-Cata-[n]diamantanes. Upper panel in red: cyclo-zz-cata[10]diamantane, and the plot of the strain energy per diamantane unit versus n^{-2} . Lower panel in blue: zz-cata[28]14amantane (front and side views with dualists), and the plot of the strain energy per unit versus n^{-1} . For structures, the c

SWB-tension and total energy per diamantane unit versus $1/n^2$ for cyclic aggregates, and versus $1/n$ for acyclic aggregates, respectively.

Zigzag Regular Poly[12...]*catamantanes*

By continuing the zigzag alternation (abbreviated as zz) for poly[12...]*catamantanes*, one obtains a quasi-linear *catamantane* structure. We do not consider assemblies of odd numbers of adamantane units as representing true zigzag [12...]*polymantanes*, so that we examine here only zz-cata[n]*diamantanes*, having n *diamantane* units or $2n$ *adamantane* units. The corresponding zz-cyclo-

cata[n]*diamantanes* (an example is shown in Figure 6) have a nice symmetry. The molecular formula of acyclic cata[n]-*diamantanes* is $C_{8n+6}H_{8n+12}$, whereas their partitioned formula is $C_{2n-2}(CH)_{4n+4}(CH_2)_{2n+4}$. Cyclo-cata[n]*diamantanes* have molecular formula $C_{8n}H_{8n}$, and partitioned formula $C_{2n}(CH)_{4n}(CH_2)_{2n}$.

As seen in Tables 1 and 2, for each new C_8H_8 *diamantane* unit the PM6-computed energy increases by 1090 kcal/mol, and the MM2-calculated strain energy for acyclic chains by 9.1 kcal/mol.

Unlike the aggregation examined in the preceding section, the straight line representing the ratio between

Table 1. Acyclic regular zz-cata[n]*diamantanes*

n	PM6-Energy	Stretch	Bend	Stretch-Bend	Torsion	Non-1,4 VDW	1,4 VDW	Strain Energy
4	-3078.1	2.4	0.8	0.1	27.5	-9.6	24.2	45.4
6	-4167.7	3.4	1.1	0.2	40.2	-14.7	33.6	63.8
8	-5257.4	4.4	1.3	0.3	52.8	-19.8	43.1	82.1
10	-6347.3	5.4	1.6	0.3	65.5	-24.9	52.5	100.5
12	-7436.7	6.4	1.9	0.4	78.2	-30.0	62.0	118.8
14	-8516.2	7.3	2.2	0.4	90.9	-35.1	71.5	137.1
24	-13974.6	12.2	3.6	0.7	154.2	-60.7	118.7	228.8
26	-15064.3	13.2	3.9	0.8	166.9	-65.8	128.2	247.2
28	-16153.9	14.2	4.2	0.8	179.6	-70.9	137.7	265.5

Table 2. Cyclic regular zz-[12...]cata[n]mantanes

n	Total-Energy	Stretch	Bend	Stretch-Bend	Torsion	Non-1,4 VDW	1,4 VDW	SWB Energy
38	-20656.4	229.7	293.7	40.2	267.6	9.1	276.7	1116.9
42	-22839.7	203.6	273	36.4	290	-14.9	287.9	1075.9
46	-25022.3	183.9	255.1	33.4	312.9	-36.1	299.9	1049.1
50	-27204.5	168.8	239.4	30.9	336.4	-55.2	312.8	1033.1
54	-29386.3	157	225.6	28.8	360.1	-72.7	326.4	1025.2
58	-31567.8	147.7	213.4	27.1	384.1	-88.9	340.6	1023.9
62	-33749.1	140.2	202.4	25.6	408.3	-104.1	355.3	1027.7
66	-35930.2	134.2	192.6	24.3	432.6	-118.6	370.5	1035.7
70	-38111	129.3	183.8	23.1	457.1	-132.4	386.2	1047
78	-42472.2	122.1	168.7	21.2	506.3	-158.7	418.4	1077.9

tension energies of acyclic zz-cata[n]diamantanes and n values exhibits a positive slope when plotted versus n^{-1} as seen in Figure 6. A tendency to relax ε_{end} to be less than ε_{in} is seen in that an internal unit is under tension from neighbor units on both sides (rather than just a single unit neighboring to an end unit). An energy cost for ε_{end} over ε_{in} is identifiable when the end unit involves a greater number of atoms and bonds to undergo interactions than appear in the (then smaller) internal units. Thus the sign of the slope for E'_n/n in our plots depends on the balance between these two counter-vailing tendencies. As indicated earlier, zigzag dualists give rise to the most compact arrangement of adamantane units, having their carbon atoms almost as in the diamond lattice. This may be the reason why in this case we have $\varepsilon_{in} < \varepsilon_{end}$.

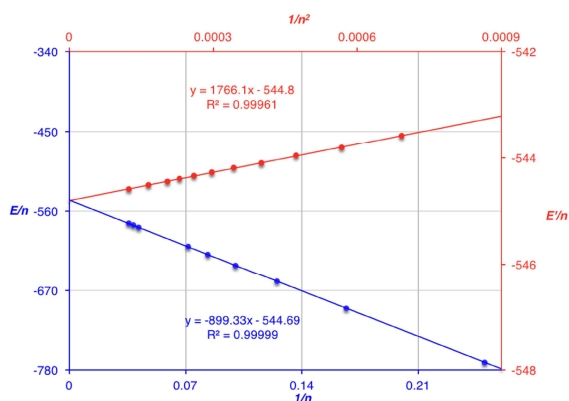


Figure 7. Upper plot in red: total energy per adamantane unit versus n^{-2} for cyclo[12...]adamantanes. Lower plot in blue: total energy per unit versus n^{-1} for acyclic [1234]-helix-[n]adamantanes.

Interestingly, with increasing n values, the so-called “non-1,4-Van der Waals” SWB-stress energies of cyclic zz-cata[n]diamantanes decrease and then change sign around $n = 40$ becoming negative at higher n values. The minimal values of 1,4-VDW and SWB tension energies correspond to $n = 37$ and 58, respectively.

Blade-perimantane

If the dualist has vertices corresponding to the carbon atoms in an *all-anti*-perhydro- k -acene, then the diamondoid is a “blade perimantane”. The dualist of its dualist leads to the zig-zag regular poly[12...]catamantane examined in the preceding section.

Acenes such as anthracene, ($k = 3$ benzenoid rings), tetracene, ($k = 4$ benzenoid rings), etc. have $n = 4k + 2$ carbon atoms, and therefore for this class of perimantanes we will discuss only integer k values. This same number

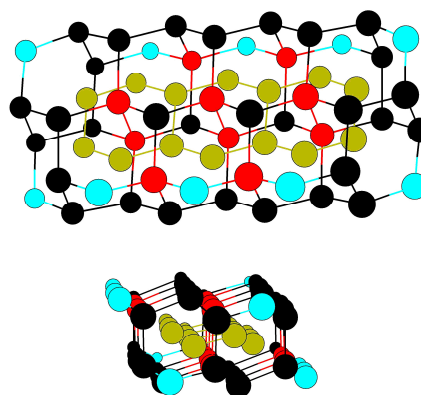


Figure 8. The blade-perimantane with its dualist for $k = 3$ (*all-trans* perhydroanthracene).

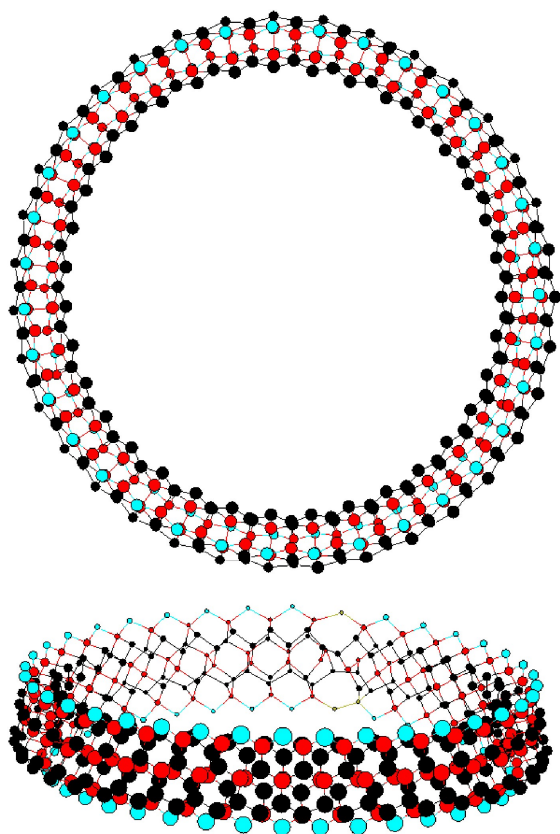


Figure 9. Two views of a cyclic blade polyadamantane.

$n = 4k + 2$ corresponds to the adamantane units in blade perimantanes. The molecular formulas of blade perimantanes are $C_{12k+4}H_{10k+6}$, and the partitioned formulas are $(CH_2)_{2k+4}(CH)_{6k+2}C_{4k-2}$. Figures 7–10 present blade perimantanes and the corresponding diagrams.

Unlike polycyclic benzenoids, whose dualists have triangles, hexagon-sharing diamondoids are self-dual, in that their dualists have vertices that reproduce on the diamond lattice. The zigzag poly[12...]catamantanes have as dualist a path with symbol [12...]. In turn, the blade perimantanes have as dualist an assembly of virtual vertices reproducing the carbon atoms of zigzag poly[12...]catamantanes.

Like the preceding zz-catamantanes, blade perimantanes contain most of their carbon atoms in a compact

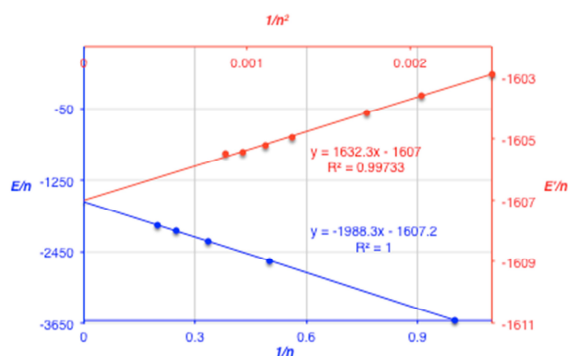


Figure 10. Upper panel in red: cyclic blade-perimantane and the plot of the Total energy per adamantane unit E/n^{-1} versus n^{-2} . Lower panel in blue: acyclic blade-perimantane and the plot of the total energy per unit versus n^{-1} .

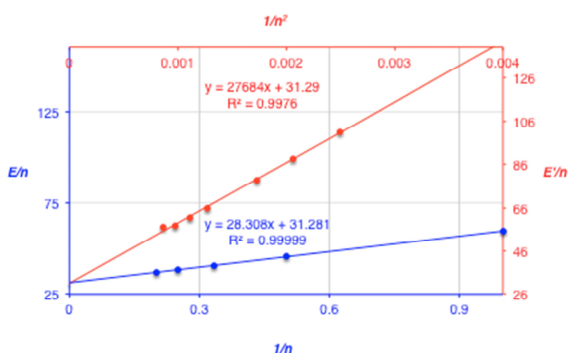


Figure 11. SWB-Tension energies (in kcal/mol) for blade-perimantane. Upper plot in red: cyclic blade-perimantane. Lower plot in blue: acyclic blade-perimantane, and the plot of the SWB-tension energy per adamantane unit versus n^{-2} .

arrangement, close to that present in the diamond net, and this is probably the explanation for the difference of SWB strain between Figures 6 and 9 on one hand (slopes with the same sign), and Figure 4 on the other hand (slopes with opposite signs) (Figure 11, Tables 3–4).

CONCLUSIONS

In Part 1 we presented one class each of cyclic and acyclic strings of regular catamantanes sharing hexagons of n

Table 3. Acyclic blade-perimantanes

n	PM6-Energy	Stretch	Bend	Stretch-Bend	Torsion	Non-1,4 VDW	1,4 VDW	Strain Energy
1	-3595.5	3.0	0.7	0.1	38.1	-12.6	30.3	59.6
2	-5202.7	4.5	1.1	0.2	61.3	-21.6	45.5	91.0
3	-6809.9	6.0	1.4	0.3	84.5	-30.7	60.7	122.2
4	-8417.1	7.4	1.8	0.3	107.8	-39.8	75.9	153.4
5	-10024.3	8.9	2.1	0.4	131.0	-48.9	91.1	184.6

Table 4. Cyclic blade-perimantanes

<i>n</i>	PM6-Energy	Stretch	Bend	Stretch-Bend	Torsion	Non-1,4 VDW	1,4 VDW	Strain Energy
20	-32058.0	437.1	540.8	75.7	497.1	-4.4	473.1	2019.4
22	-35279.3	384.5	506.2	68.1	540.1	-45.1	492.1	1946.0
24	-38499.6	344.9	475.3	62.1	583.8	-81.4	512.1	1896.7
28	-44938.1	291.1	422.6	53.0	672.6	-144.7	554.4	1849.0
30	-48156.5	272.5	400.1	49.6	717.4	-173.0	576.8	1843.4
32	-51374.4	257.2	379.9	46.6	762.5	-199.6	600.3	1846.8
34	-54586.1	254.9	397.2	45.4	810.1	-220.7	647.8	1934.7

adamantane units in a chiral helical arrangement.^[5] The diagrams of SWB tension energy per adamantane unit versus $1/n^2$ for cyclic aggregates, and versus $1/n$ for acyclic aggregates, respectively, manifest slopes with opposite signs, and this proved to be true for most other hexagon-sharing aggregates (unpublished data). In our search, however, we have encountered two exceptions with slopes of the same signs, discussing these exceptions in the present paper – with a central part of the understanding by distinguishing between a geometric strain energy, and the SWB tension energies. Other cases of actual strain in related nanostructures reveal^[11,12] this distinct signature.

REFERENCES

- [1] J. E. Dahl, S. G. Liu, R. M. Carlson, *Science* **2003**, *299*, 96.
- [2] G. A. Mansoori, P. L. Barros de Araujo, E. S. de Araujo, *Diamond Molecules with Applications in Biomedicine, Materials Science, Nanotechnology and Petroleum Science*, World Scientific, Singapore, **2012**.
- [3] H. Schwertfeger, A. A. Fokin, P. R. Schreiner, *Angew. Chem. Int. Ed. Engl.* **2008**, *47*, 1022.
- [4] K. E. Drexler, *Engines of Creation. The Coming Era of Nanotechnology*, Anchor Books, Garden City, NY, 1986.
- [5] A. T. Balaban, D. Bhattacharya, D. J. Klein, Y. P. Ortiz, *Internat. J. Quantum Chem.* **2016**, *116*, 113.
- [6] A. T. Balaban, P. v. R. Schleyer, *Tetrahedron* **1978**, *34*, 3599.
- [7] A. T. Balaban, F. Harary, *Tetrahedron* **1968**, *24*, 2505.
- [8] V. Prelog, R. Seiferth, *Ber. Dtsch. Chem. Ges.* **1941**, *74*, 1464.
- [9] A. T. Balaban, K. B. Chilakamarri, D. J. Klein, *J. Math. Chem.* **2009**, *45*, 725.
- [10] P. v. R. Schleyer, J. E. Williams, K. R. Blanchard, *J. Am. Chem. Soc.* **1970**, *92*, 237.
- [11] L. L. Griffin, J. Wu, D. J. Klein, T. G. Schmalz, L. Bytautas, *Internat. J. Quantum Chem.* **2005**, *102*, 387.
- [12] D. Bhattacharya, D. J. Klein, J. M. Oliva, L. L. Griffin, D. R. Alcoba, G. E. Massaccesi, *Chem. Phys. Lett.* **2014**, *616–617*, 16.
- [13] D. Bhattacharya, Y. Ortiz, D. J. Klein, *Chem. Phys. Lett.* **2016**, *647*, 185.
- [14] Y. Ortiz, D. Bhattacharya, D. J. Klein, J. F. Liebman, *Rev. Roum. Chim.* **2016**, *61*, 269.